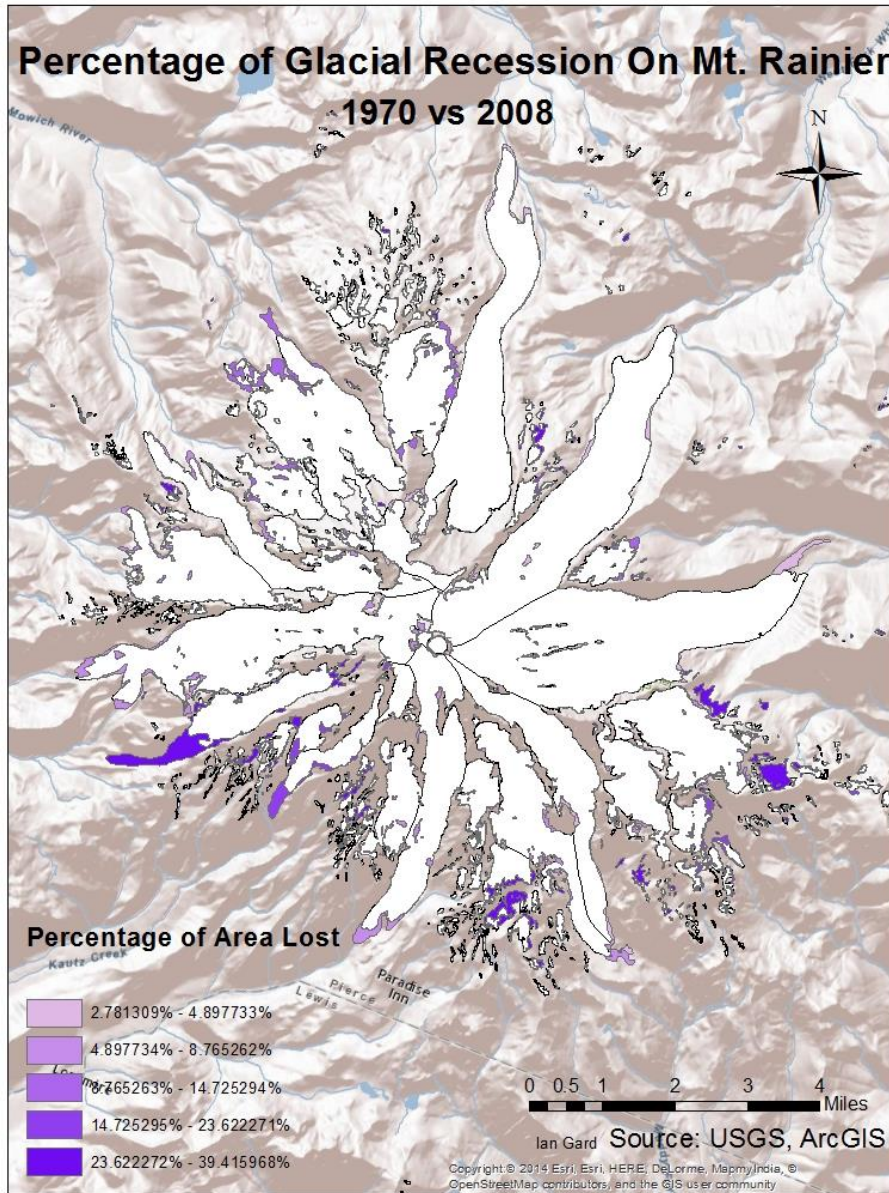


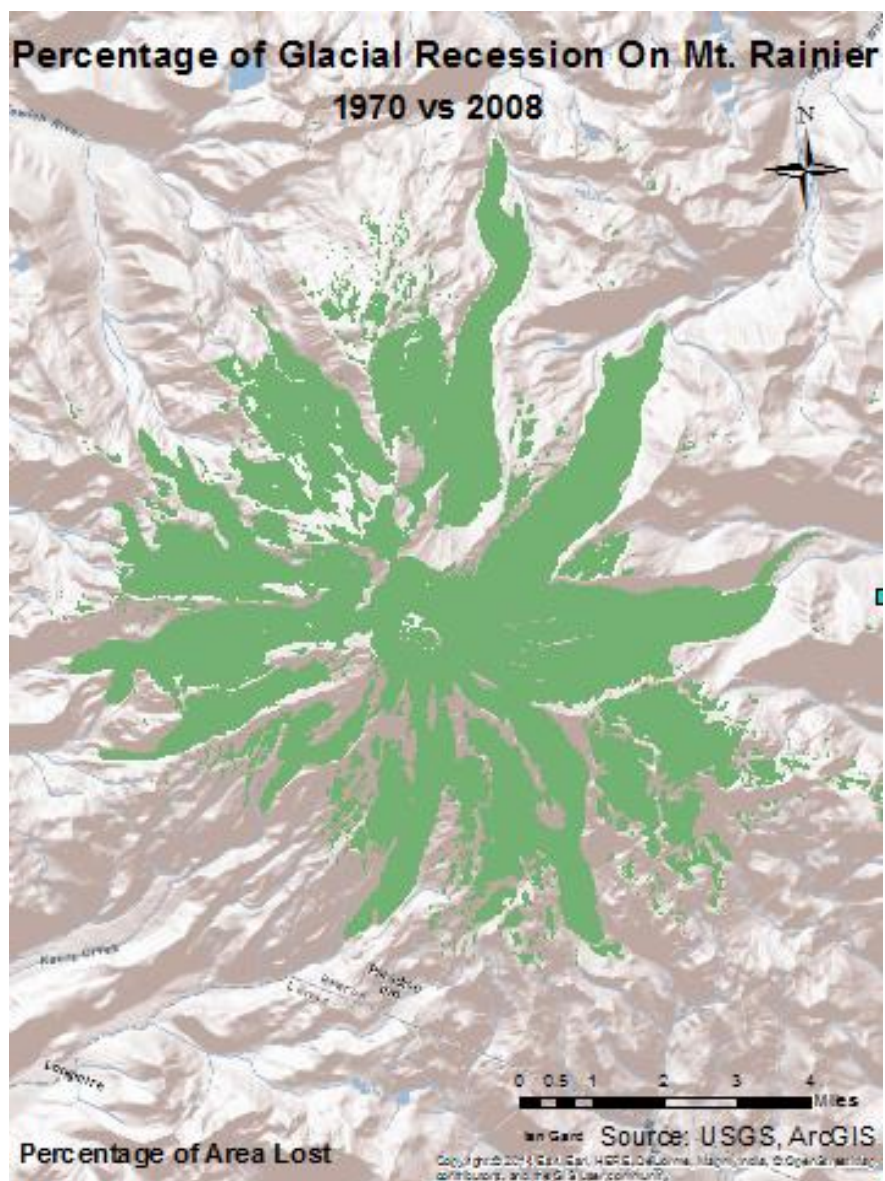
Dekalb Taylor Municipal Airport 5 MW Solar PV Site Layout

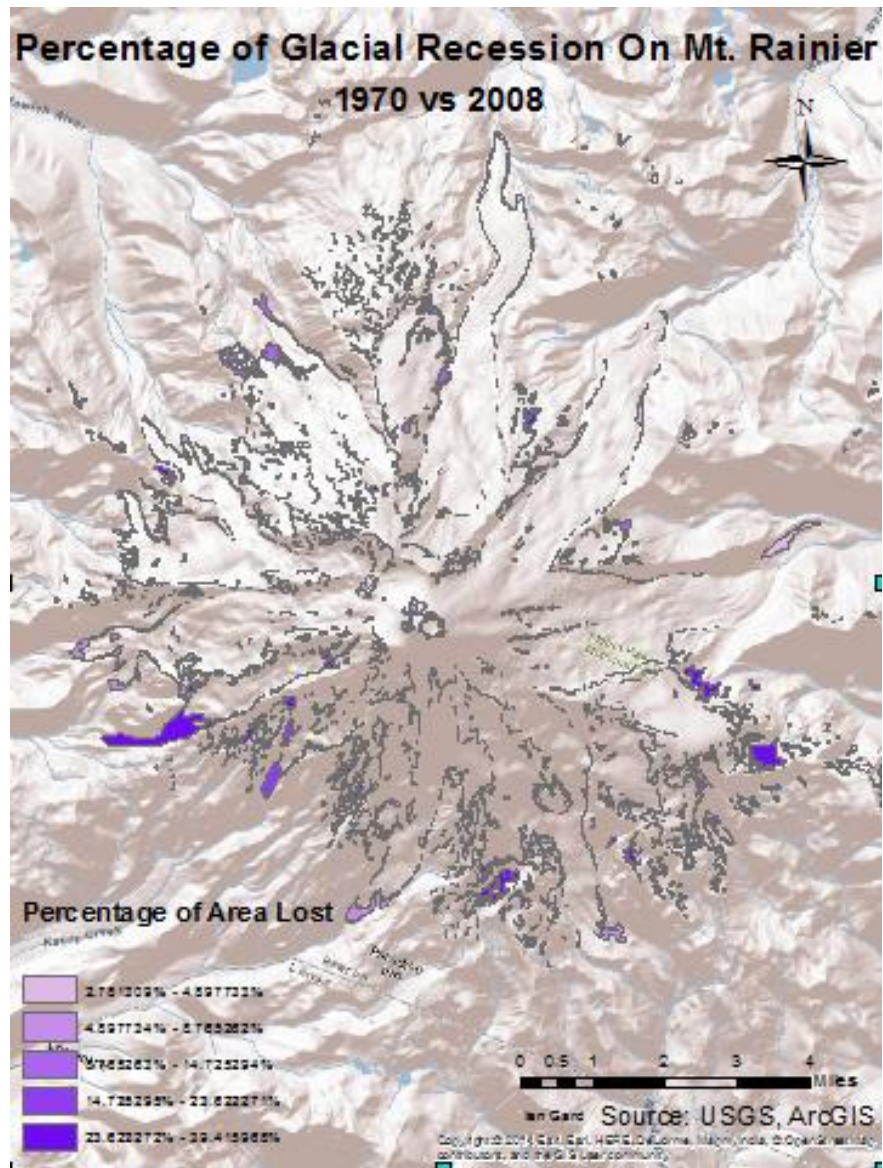


An original final project I planned and produced for the course Introduction to GIS. Highlights glacial changes of Mt. Rainier using the software program ArcMap.

The first map displays the final results of the project, demonstrating the areas of lost glacier between 1970-2008 while also representing the full extent of glacier in 1970. The second displays the total extent of glacier in 1970 without comparison for reference. While the bottom map is a clearer view of the areas of lost glacier without being skewed visually by glacial extent from 2008.







This project aimed to explore the spatial areal/snowfield recessional patterns on Mt. Rainier specifically between the dates of 1970 and 2008. Asking the research question, what are the patterns of glacial recession within this time frame? Understanding glacial areal recessional patterns in glacierized areas assists the continued understanding and research of changing climatic conditions and impacts in these, usually hypersensitive areas. Helping to concentrate efforts in area that have been experiencing the most intensive changes in maximum extent.

Polygon extent of glacial maximum from LiDAR imaging from an area survey taken by the National Park Service in during 2007-2008, released publicly by the USGS was used. With these polygons being overlayed on a shaded relief base map provided by ArcGIS.

Once the data was gathered and inserted into ArcMap I overlayed these figures. In order to isolate the individual polygons representing the 1970s-glacial extent from the 2008 extent. In order to perform this operation the Overlay Erase tool was used under the Analysis Tools section of ArcToolbox. Then attribute fields of the original area and the new area of the output layer were compared and a new attribute field was created in order to show the total difference in area, which was then converted to percentages, which are represented on the map.

The full range of percentages lost per polygon range from 2.78%-39.41%. The entirety of the original area of the 1970s glacial extent was measured at 93,278,099 square meters, with the total of lost area by 2008 being measured at 9,433,949 square meters. Equating to roughly ten percent of the total glacial/snow extent being lost in the last thirty eight years. The measured polygons with the highest percentage of area lost is as follows; Snowfields-39.41%, Van Trump Glacier- 34.76%, Pyramid Glacier- 33.68%, Paradise Glacier- 32.72%, Williwakas Glacier-31.34%.

The data suggests a higher percentage of recession along the southern part of the mountain and historic glacier extent. Factors such as lower elevation, increased risk of flooding and effect of runoff, rainshadow, decreased albedo, higher relative humidity, and surface temperatures due to anthropogenic influences likely all play factors in the areal concentration of this recession. An interesting aspect of the individual polygon percentage lost is the comparison between snowfields and glaciers. Snowfields lost the largest percentage of area, which is to be expected due to the snows sensitive nature to changes in weather and climate. However, the Van Trump Glacier, the glacier with the largest percent of lost area, was only measured as about attaining about 5% more of its total area. This is an alarmingly low difference when comparing the nature of snow to glaciers, and demonstrating the sensitivity in glaciers to increasing climate variability.

Presenting the areas in percentages versus meters on the map is a superior format for public communication in order to display the urgency of the extent recession. The more public knowledge on the subject can assist in increased funding to the national park system and other environmental conservation agencies.

ArcGIS. 2009. World Shaded Relief.

<https://www.arcgis.com/home/item.html?id=9c5370d0b54f4de1b48a3792d7377ff2>

Robinson, J.E., Sisson, T.W., and Swinney, D.D., 2010, Digital topographic map showing the extents of glacial ice and perennial snowfall at Mount Rainier, Washington, based on the LiDAR survey of September 2007 to October 2008: U.S. Geological Survey Data Series 549 [<https://pubs.usgs.gov/ds/549/>].

<https://www.arcgis.com/home/item.html?id=c61ad8ab017d49e1a82f580ee1298931>

<https://www.arcgis.com/home/item.html?id=c61ad8ab017d49e1a82f580ee1298931>

Change Detection Analysis of the Hubbard Glacier

Introduction.

The image-processing objective of this project consisted of the attempted change detection analysis of the Hubbard Glacier through ENVI classic 5.3. The Hubbard Glacier is a glaciated area covering parts of eastern Alaska, spilling over into Yukon, Canada, two hundred miles northwest of Juneau. The glacier face can reach heights of four hundred feet and is more than six miles wide where it meets the ocean, the specific area of interest for this analysis. I found the Hubbard Glacier to be an intriguing area of interest due to its atypical, active growth patterns. There have been two major growth surges of the glacier in the last thirty years, in May of 1986 the glacier grew and ended up blocking the Russel fjord creating a lake. This actually presented some problems for the surrounding area. Threatening to flood the nearby town of Yakutat, Alaska. Sea level rose within the blocked off fjord, raising it by over eighty feet. This glacier runoff began to dilute the salinity of the water and threatened native sea life. On October eighth, this natural dam gave way and ensued a massive glacial lake outburst flood. With its peak discharge of water equating to 3,970,000 liters a second of water. The glacier again surged in June of 2002, once again blocking the entrance of the fjord. The new dam ended up breaking in August of the same year. This time caused by rain causing the water level to overflow the glacial dam and cause major erosion to the moraine. And causing yet another massive glacial lake outburst flood, causing a peak discharge of 1,850,000 liters of water a second. Both of these dam failures are the largest glacial lake outburst floods recorded.

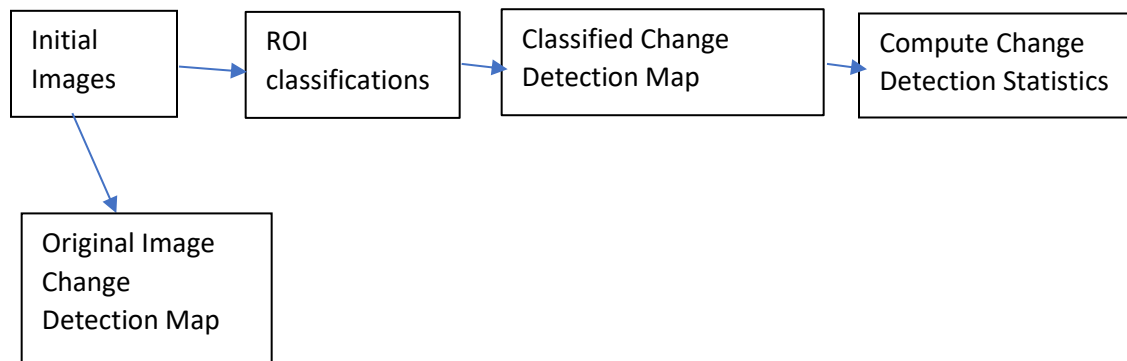


Figure 1: Hubbard Glacier, Alaska

I was interested in the biophysical materials of the glacial ice, water, vegetation, and bare ground of the surrounding area. All are important physical features in differentiating the differences in the change and growth of the glacier. The remote sensing data appropriate to collect were Landsat satellite imagery of the glacier in different years to compare glacial changes. I specifically wanted to look at the initial glacial change between May third of 1985 and September eleventh of 1986. 1985 being a year the glacier was not blocking the fjord and 1986 being a year it did. Landsat 4-5TM was the

satellite collecting data during this time-period. The imagery of this satellite is taken 60m spatial resolution. The glacier surged and retreated at different times of the year, so images from different years and different months had to be used, seasonal variance had to be taken into account.

Methods.



The image processing objective was directly derived from the change detection tool available in Envi. This was in inspiration for the objective, put within an environmental context. The process of the experiment began with the collection of Landsat satellite imagery. The two images of glacier taken from earth explorer from 1985 and 1986 were uploaded into Envi classic 64 bit. These were displayed with the bands 4,3,2. First I wanted to explore the change between the two original images. I processed a change detection map of the two images unchanged from their original band uploads. Next I wanted to look at more specific change between all of the aspects of the images. To do this I classified water, ice, vegetation, and the bare ground of the images with the region of interest tool. I then went to attempt to create a more specific change detection image. I had to choose a single band from each image, one from 1985, displaying the "initial" state, and one from the 1986 image representing the "final" state. The change type was set to simple difference. This simply subtracted the initial state image from the final state image. And normalization was the option chose from the data pre-processing options. This took the image minimum and divided it from the overall image range. This was then saved to a file and resulted in a difference map. The map is color coded with darker shades of red representing more intense positive change and darker blue representing more extreme negative change. Gray indicated little to no change. Next I wanted a more statistical analysis of the change detection image I had just computed. This was achieved through the change detection statistics tool. I again chose a single band from the initial, 1985, image and final, 1986 image. Equivalent classes then had to be paired, and each of the same ROI classifications were matched from each of the images. The option of what statistics would be displayed were shown, I chose percent. This tool also allowed classification masks to be created and these were saved to files and created. Envi then created a change statistics report.

Results.

The computed change detection map (figure 3/4) highlighted a change in ice blocking the fjord between the two years. However, the map produced was a bit confusing and displayed changes in pixels such as water that hadn't changed, especially in the specific area I was observing. A large change in vegetation was highlighted as well. The original image change detection map (figure 2) computed,

highlighted a clear, less noisy difference in glacial growth in the fjord between the two years. The change detection statistics suggested a different picture. Depicting ice change into bare ground and vegetation, rather than melting into water. I did not take the unclassified percentage data into account when comparing the statistics. The largest in change in classes from the initial ice other than to final ice, were bare ground and vegetation. It appeared the ROI classifications were not incredibly clear and ended up including a sizeable amounts of pixels in wrong classes.

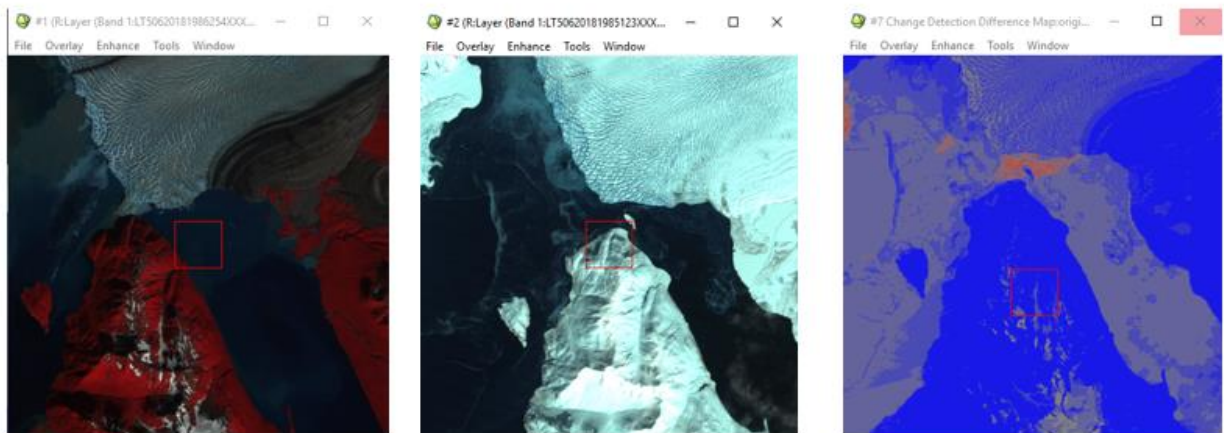


Figure 2: Original Image Change Detection Map

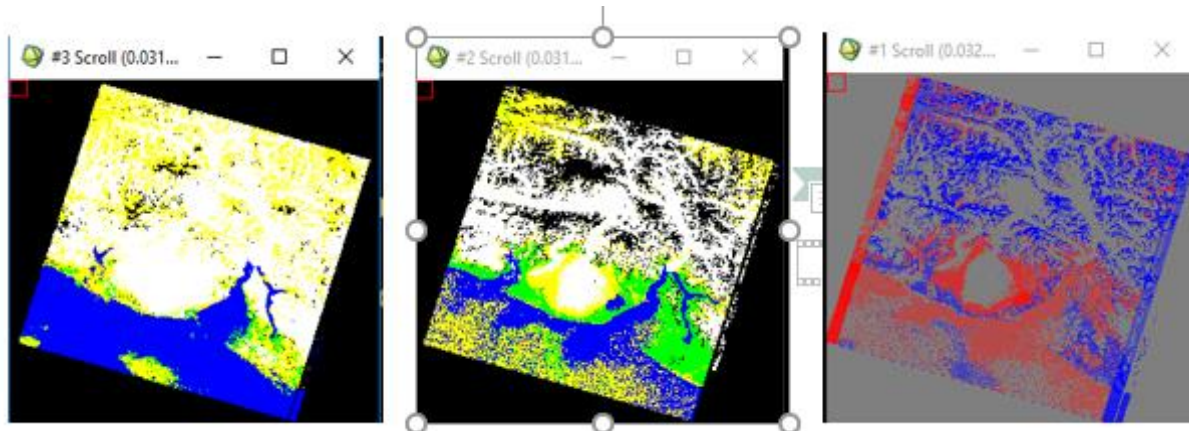


Figure 3: Classified Change Detection Map (Full Image)

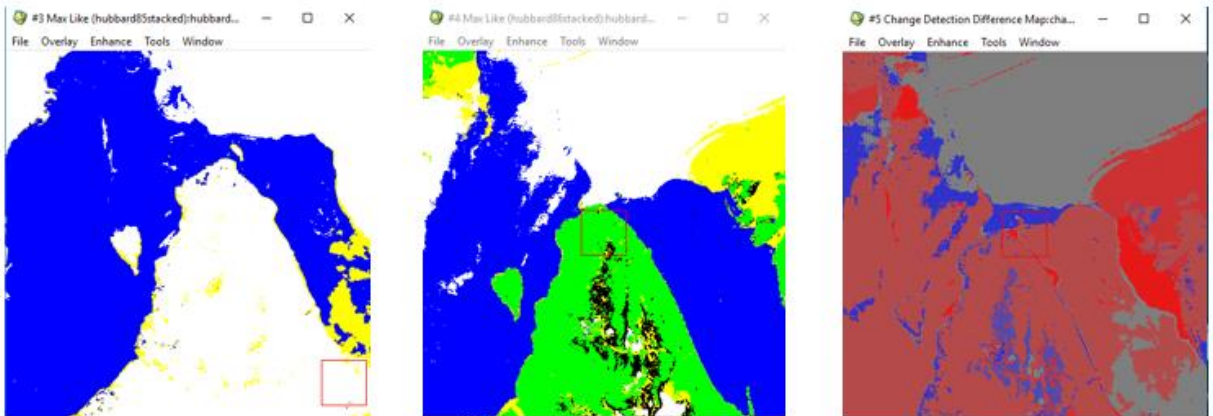


Figure 4: Classified Change Detection Map

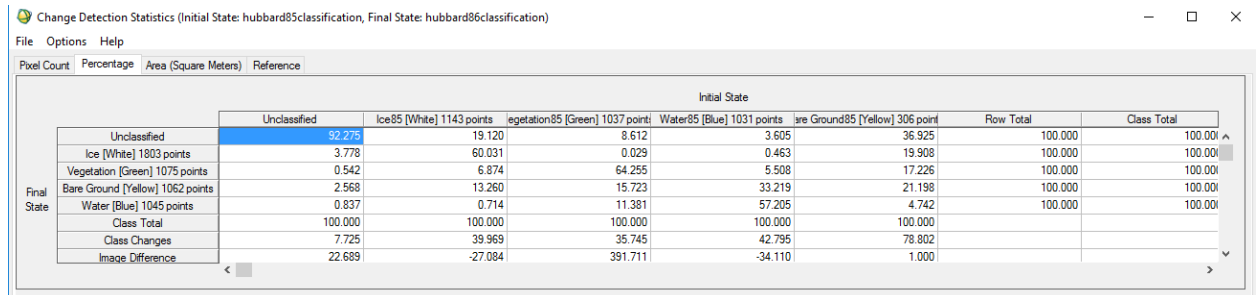


Figure 5: Change Detection Percentage Statistics

Discussion.

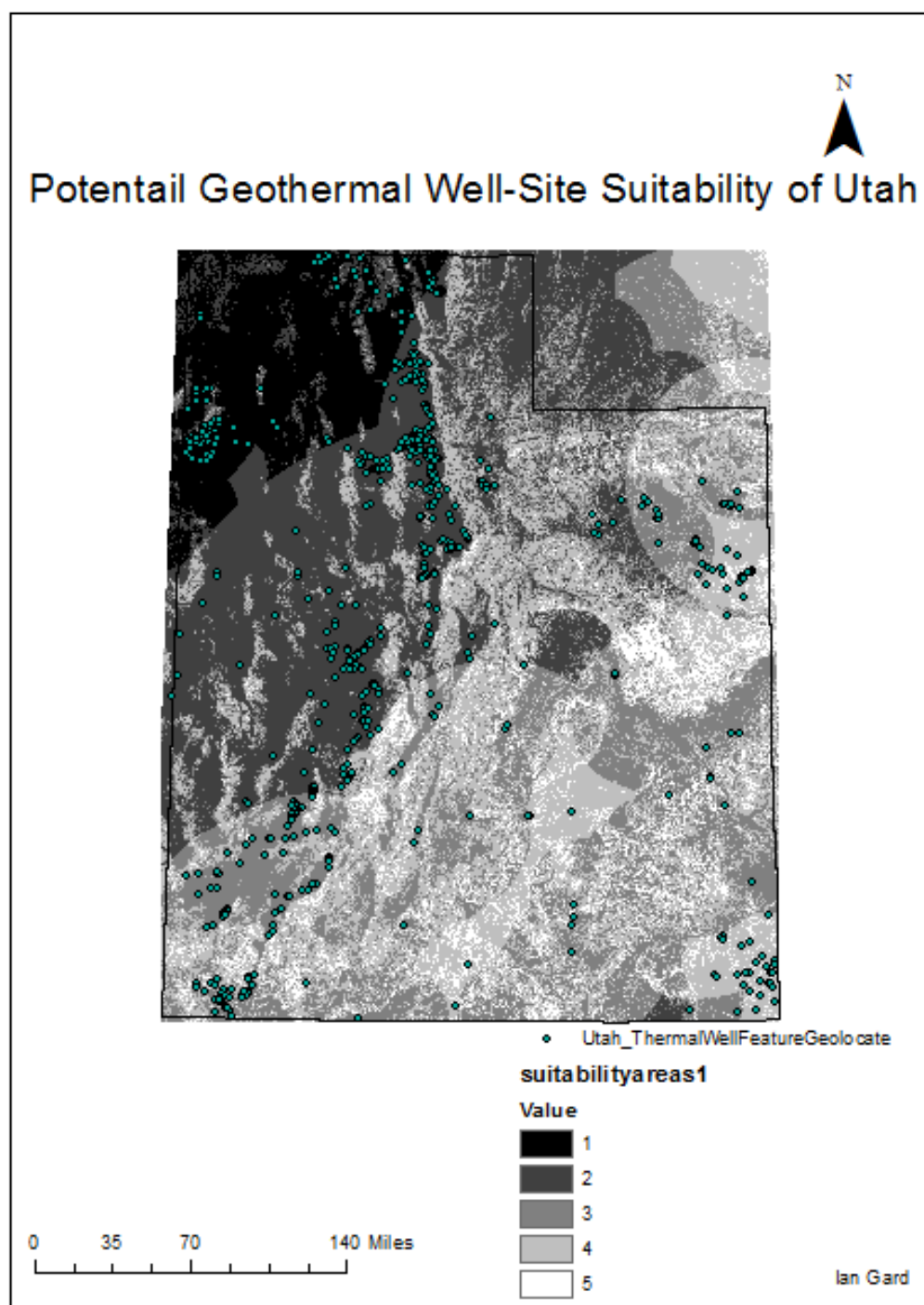
Overall the classification of the images could have been much more accurate, this was due to user error when trying to define the ROIs. The initial difference map before user classification presented a much clear image of the glacial growth at the mouth of the Russell fjord. The second, classified change detection map showed change in pixels that had actually changed, for example water to bare ground. The change detection statistics actually made the result more confusing. I expected ice to mostly change to water, specifically thinking of the glacier interacting with the fjord. However, ice mostly changed to vegetation and bare ground, with thirteen percent changing to bare ground and six percent changing to vegetation. I believe what this was demonstrating was a reduction in snow cover, rather than glacial ice. These two glacial features were not taken into consideration at the beginning of the project. There was not really a way to differentiate these pixels when classifying the ROIs by hand so reduction of growth in glacial ice and simple snow cover, something that is much more variable with seasonality, was not taken into account. Due to the difference in seasons of each images this played a major role in computing the percentage of change for each class. This can clearly be seen in the classified change detection image map. Overall what this classification seem to do was actually measure the change in overall snow cover between the two years and did not highlight the change in glacial growth statistically. No accuracy assessment was done with the classifications, was there was no way of knowing exactly how accurate the ROIs ended up being. Visually for the whole images they definitely could have been significantly more accurate.

In retrospect, the processing objective was difficult to complete accurately with the tools used. Comparing images from different years, and especially from different seasons created results that were not necessarily reflective of what the initial objective, specifically looking at glacial growth affecting the Russel fjord, was intended to do. Attempting an objective of possibly observing overall snow cover of an area from different years, but from the same seasonal timeframe. Change detection in this context may very well show a more complete and accurate picture.

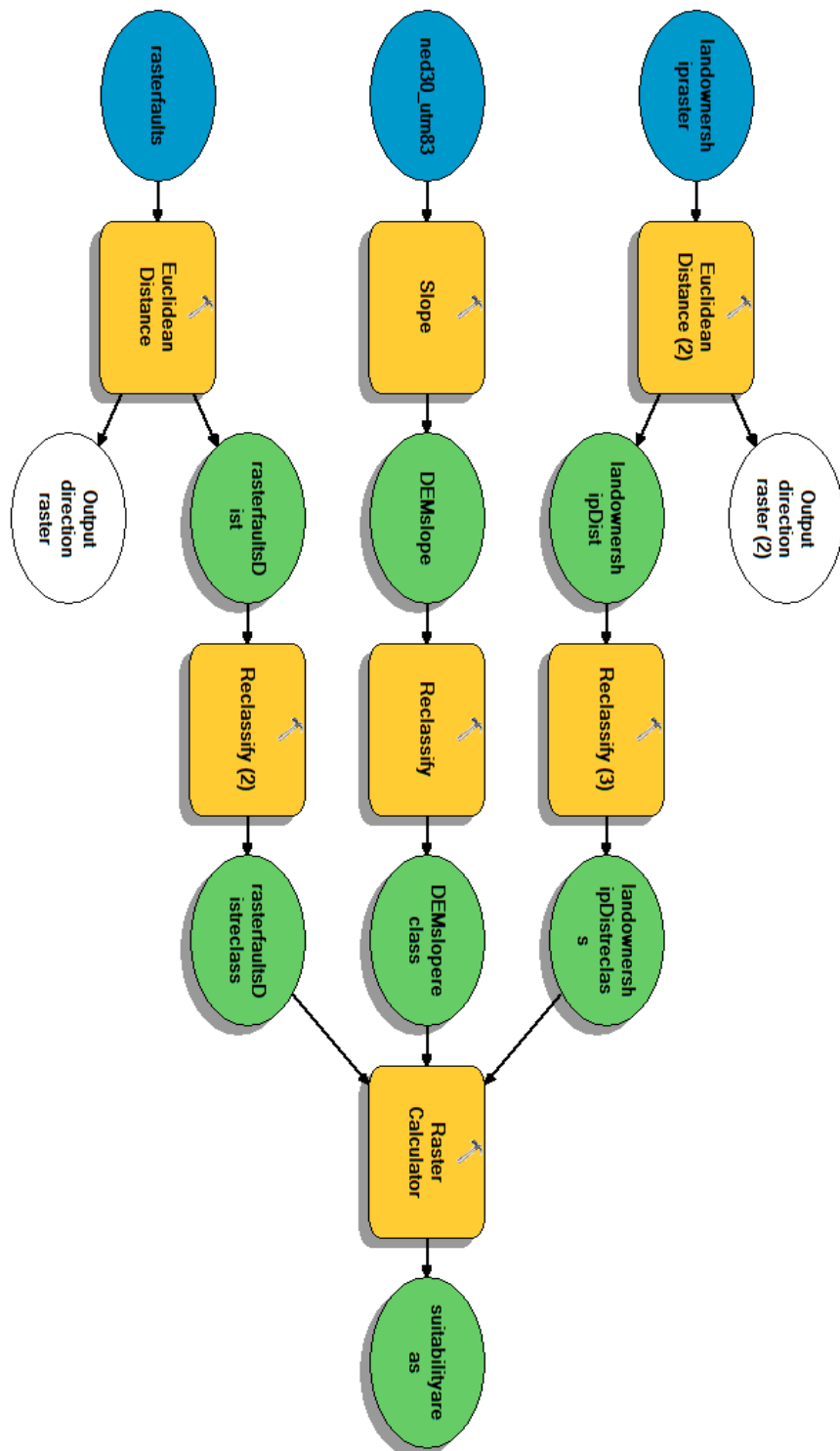
References

- Change Detection Analysis. (n.d.). Retrieved May 10, 2017, from <https://www.harrisgeospatial.com/docs/ChangeDetectionAnalysis.html>
- D.C. Trabant, R.S. March, D.S. Thomas. (n.d.). Hubbard Glacier, Alaska: Growing and Advancing in Spite of Global Climate Change and the 1986 and 2002 Russell Lake Outburst Floods. Retrieved May 10, 2017, from <https://pubs.usgs.gov/fs/fs-001-03/>
- Moran, E., Brondizio, E., Mausel, P., & Lu, D. (2010). Change Detection Techniques . International Journal of Remote Sensing, 2365-2401. Retrieved from <http://www.tandfonline.com/doi/full/10.1080/0143116031000139863?scroll=top&needAccess=true>
- Rignot, E., & Zyl, J. V. (1993). Change detection techniques for ERS-1 SAR data. IEEE Transactions on Geoscience and Remote Sensing, 31(4), 896-906. doi:10.1109/36.239913

Geothermal well-site suitability project of Utah and the surrounding area. Created based on the factors of slope, land ownership and proximity to potentially harmful faults. Darker areas represent more suitable land for the creation of geothermal wells.



Geothermal Well Site Suitability Analysis Workflow created with ArcGIS's ModelBuilder



Potential geothermal Well Site Suitability Analysis

For this final project, I pursued a potential geothermal well site suitability analysis. My goal was to create a suitable map indicating areas where there are high amounts of potential geothermal energy resources available within the state of Utah. This was achieved using certain input criteria concerning different aspects related to the success of constructing possible geothermal wells and power plants.

I chose my site as the state of Utah due to its location. The western United States has an incredibly high amount of geothermal energy resource potential. And Utah is the third largest geothermal energy producing state in the U.S. California leads the nation with 2,732.2 megawatts of installed geothermal energy capacity. Nevada is second with five hundred and seventeen megawatts of installed energy capacity and Utah is third with forty-eight megawatts of installed energy capacity. Even as the third largest in the nation the U.S. installed capacity is a fraction of what California and Nevada consist of. Because of this is found Utah to be a great area to conduct this analysis, an area high in potential geothermal resources, but low in resource production and development. Aggressive pursuit of this clean renewable energy source would create a substantial sector of the energy economy for the state and likely bring in large amounts of revenue.

The components of the project included initial vector points of thermal wells throughout Utah. These provided eight hundred and forty-four locations of thermal anomalies in well sites that may indicate new geothermal resources. The suitability criteria included a digital elevation model of Utah and the surrounding area, national park boundaries within the state, and quaternary faults. The DEM was used in order to find areas of lesser slope, allowing for easier construction of power plants and access to the pre-existing well sites. The national park boundaries were used in an attempt to find areas suitable for construction furthest away from national parks. These included parks such as, Zion, Canyonlands, and Arches National Park. These natural areas are incredibly sensitive and while geothermal energy is a clean renewable resource, construction of power plants and expansion of their wells systems may include pollutant processes, aspects not desired within these areas. Quaternary faults are active faults that may indicate the occurrence of concealed geothermal energy systems. These were included in the suitability criteria because proximity to these faults may increase the likelihood of geothermal resource potential.

In order to begin the project the quaternary fault and national park boundary data was to be rasterized from their original vector form. The slope of the DEM was then derived and reclassified into five classes. With the first class being the lightest colored areas representing the flattest portions of the model and the darkest the fifth class, representing intense slope. Next the Euclidean distance was derived from the national park boundaries and reclassified into five classes. The lightest portion of the classification map demonstrated the areas furthest from the national parks. Then the Euclidean distance of the quaternary faults was derived and reclassified into five classes. Unlike the national parks proximity was the priority in this classification and the dark red areas represented the class closest to them. The weighted overlay of the criteria was conducted using the raster calculator. The national parks distance layer was weighted at .5, while the quaternary faults distance and slope layers were weighted at values of .25. The last two layers were weighted less due to the original well sites pre-existing thermal anomalies and site construction, making proximity to quaternary faults and flatter surfaces more of a luxury and increased convinces than absolutely necessary. This produced a suitability output layer representing areas throughout the state of Utah that best fit the criteria of the analysis. This was also reclassified into five classes, with the darker areas representing the area's best matching the criteria. The well sites were then overlaid on this suitability output and the multi value to point tool was used in order to derive how many sites were found in each suitability class. Of the four hundred and eighty eight sites, one hundred and fifty six of these sites were located in the most suitable areas. Four hundred and twelve were located on class two, one hundred and ninety seven within class three, seventy four were in class four, and five of the sites fell within class five. Model builder was then used to display the steps taken to create the suitability map.

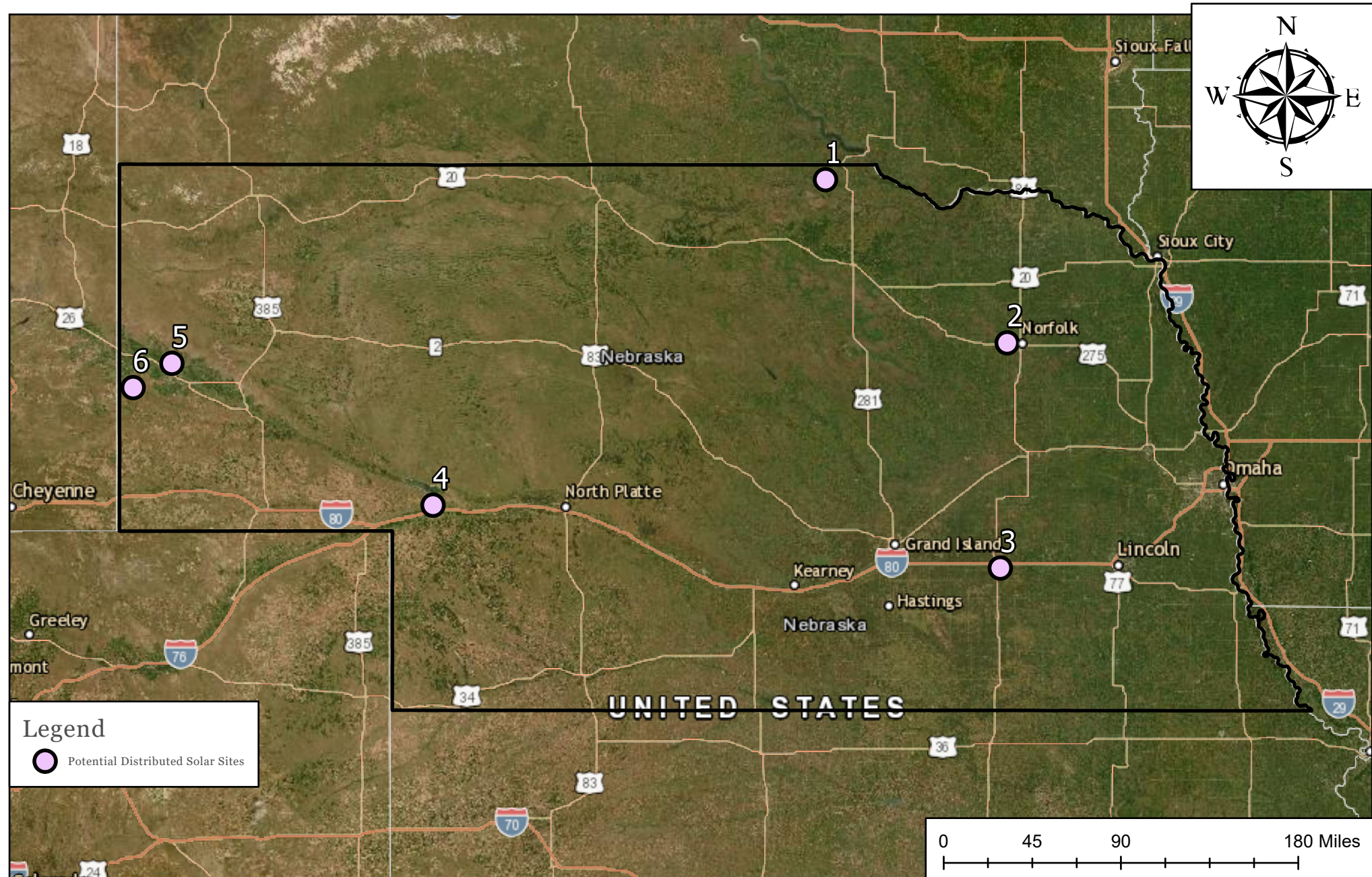
Assessing the analysis's output the well sites that fell within the most suitable areas should be further explored for their high geothermal energy potential. These sites were overall confined to the northwestern portion of the state. Throughout the analysis many more criteria factors would have been useful in refining and creating a much more accurate map for well sites with higher resource

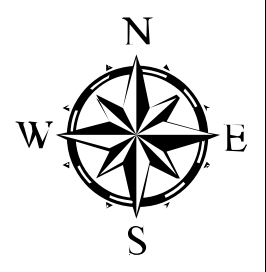
potential located on land better for development and construction. Factors such as proximity to major roads, landuse and landcover, and population density would have all made for more accurate suitability areas. More specific classification for each for the selected criteria would have also refined the analysis. For example creating classes that would have highlighted almost exclusively the quaternary faults themselves and not the general area around them.

Overall, the analysis illustrated a general area of where existing well sites with a high potential to have geothermal energy derived from them are located. More extensive analysis can be done of the subject and on this data in order to create a more specific criteria. Overall the results of this analysis give an overall idea where energy and funds should be exerted to in order to increase the state's overall geothermal energy resource producing capacity.

References

- <https://gis.utah.gov/data/sgid-cadastre/land-ownership/>
- <http://geology.utah.gov/resources/energy/geothermal/national-geothermal-data-system/>
- <http://www.deseretnews.com/article/865574271/Utah-No-3-in-the-country-for-geothermal-power.html>





Legend

- Distribution Lines
- ★ NPPD Sub
- Yellow Box Buildable Area

Project Name: Site 1 - BELF Boyd County
Butte, NE

Notes:

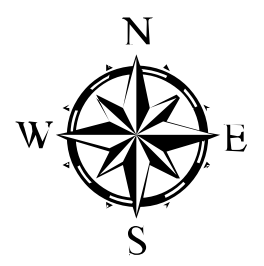
330 W. State St. Suite 1
Geneva, IL 60134
www.sunvest.com

Project Location: 42.917217, -98.853957

Date: 6/18/2021

Drawn By: I. Gard





Project Name: Site 2 - Norfolk

Notes:

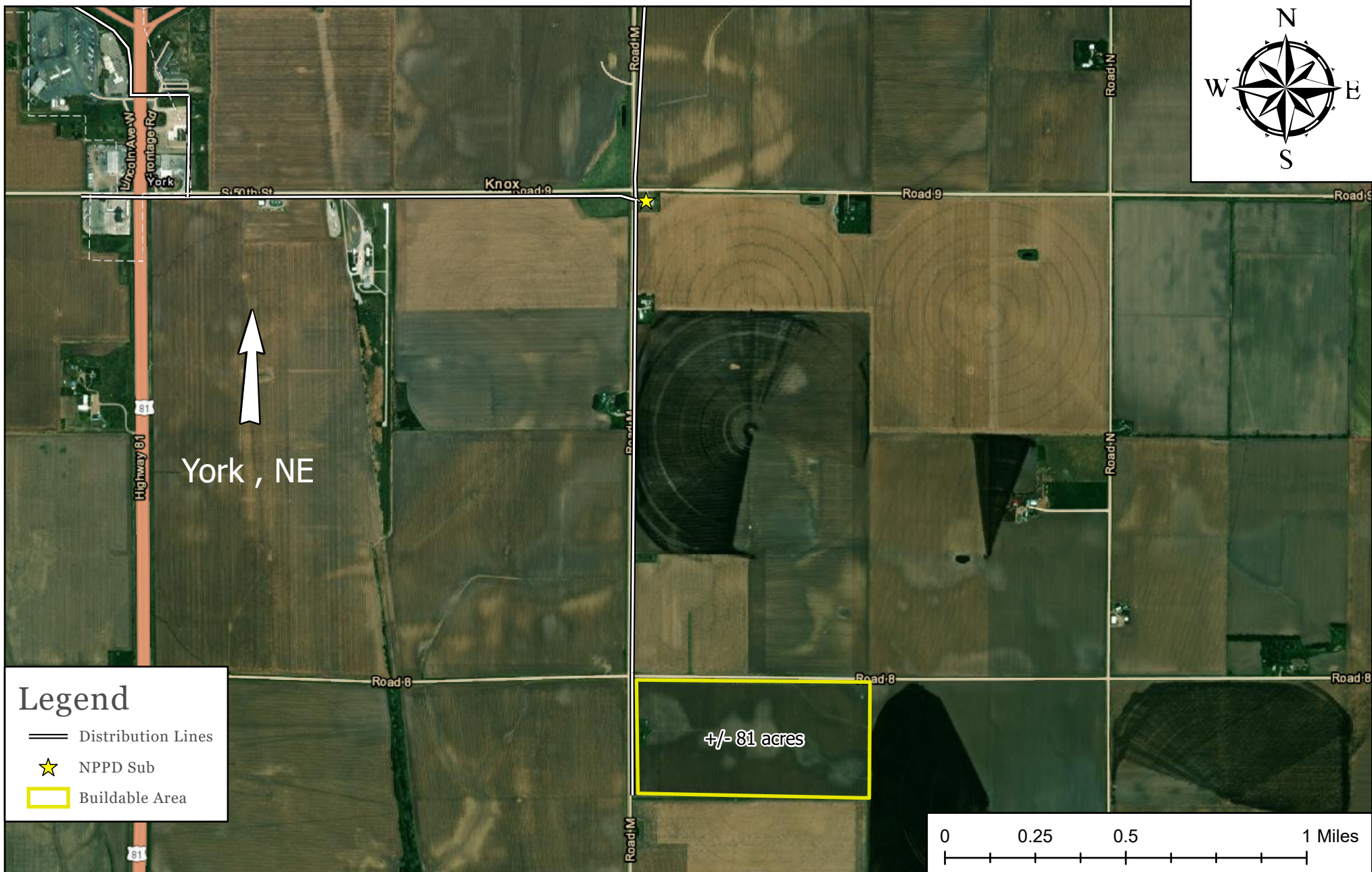
330 W. State St. Suite 1
Geneva, IL 60134
www.sunvest.com

Project Location: 42.035209, -97.522872

Date: 6/18/2021

Drawn By: I. Gard





Project Name: Site 3 - York

Notes:

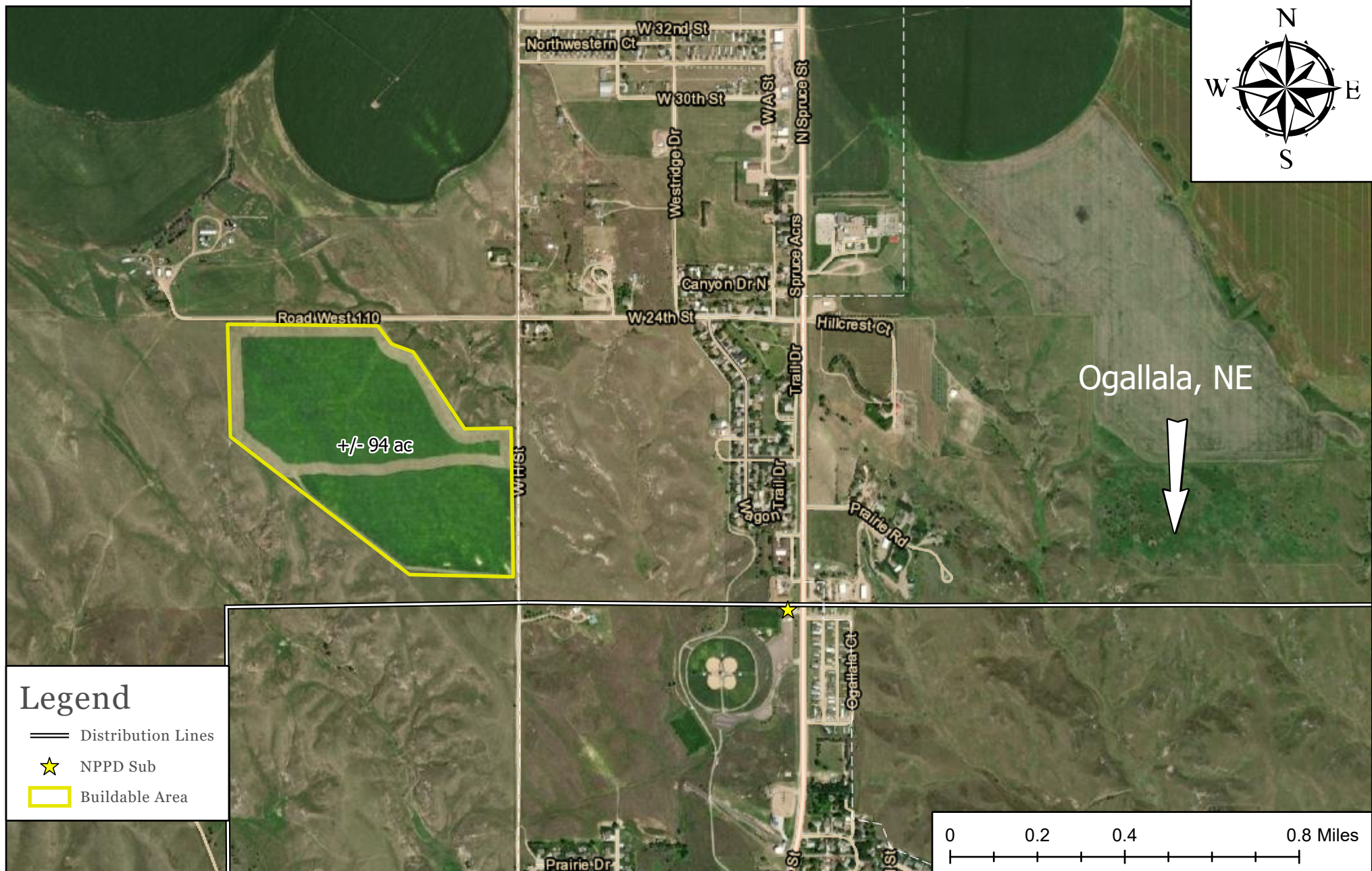
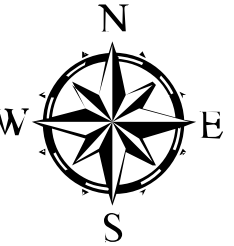
330 W. State St. Suite 1
Geneva, IL 60134
www.sunvest.com

Project Location: 40.797918, -97.573409

Date: 6/18/2021

Drawn By: I. Gard





Project Name: Site 4 - BELF Keith County
Ogallala, NE

Notes:

330 W. State St. Suite 1
Geneva, IL 60134
www.sunvest.com

Project Location: 41.147552, -101.735952

Date: 6/18/2021

Drawn By: I. Gard





Project Name: Site 5 - Scottsbluff

Notes:

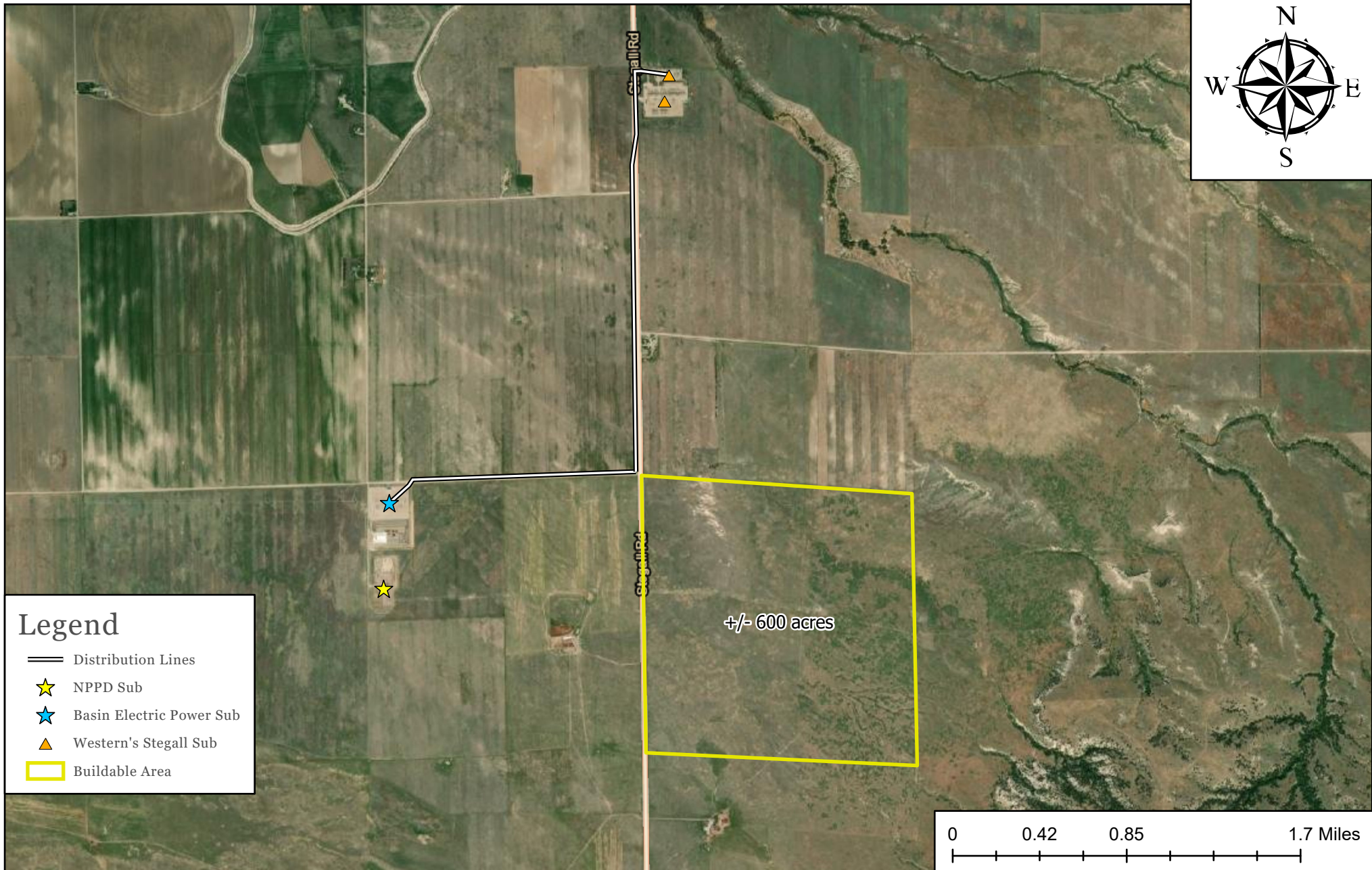
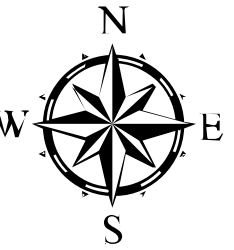
330 W. State St. Suite 1
Geneva, IL 60134
www.sunvest.com

Project Location: 41.924011, -103.650502

Date: 6/18/2021

Drawn By: I. Gard





Project Name: Site 6- BELF Scottsbluff County

Notes:

330 W. State St. Suite 1
Geneva, IL 60134
www.sunvest.com

Project Location: 41.794393, -103.939228

Date: 6/18/2021

Drawn By: I. Gard

